THE JOURNAL OF BIOLOGICAL CHEMISTRY VOL. 291, NO. 19, pp. 10399–10410, May 6, 2016

Oxidant-induced Interprotein Disulfide Formation in Cardiac Protein DJ-1 Occurs via an Interaction with Peroxiredoxin 2*[S]

Received for publication, October 22, 2015, and in revised form, March 4, 2016 Published, JBC Papers in Press, March 4, 2016, DOI 10.1074/jbc.M115.699850

Mariana Fernandez-Caggiano[‡], Ewald Schröder[‡], Hyun-Ju Cho[‡], Joseph Burgoyne[‡], Javier Barallobre-Barreiro[§], Manuel Mayr[§], and Philip Eaton[‡1]

From the [‡]King's College London, Cardiovascular Division, The British Heart Foundation Centre of Excellence, The Rayne Institute, St. Thomas' Hospital, London SE1 7EH, United Kingdom and [§]King's College London, Cardiovascular Division, The British Heart Foundation Centre of Excellence, The James Black Centre, King's College Hospital, London SE5 9NU, United Kingdom

The role and responses of the dimeric DJ-1 protein to cardiac oxidative stress is incompletely understood. H_2O_2 induces a 50-kDa DJ-1 interprotein homodimer disulfide, known to form between Cys-53 on each subunit. A trimeric 75-kDa DJ-1 complex that mass spectrometry shows contained 2-Cys peroxiredoxin also formed and precedes the appearance of the disulfide dimer. These observations may represent peroxiredoxin sensing and transducing the oxidant signal to DJ-1. The dimeric disulfide DJ-1 complex was stabilized by auranofin, suggesting that thioredoxin recycles it in cells. Higher concentrations of H_2O_2 concomitantly induce DJ-1 Cys-106 hyperoxidation (sulfination or sulfonation) in myocytes, perfused heart, or HEK cells. An oxidation-resistant C53A DJ-1 shows potentiated H_2O_2-induced Cys-106 hyperoxidation. DJ-1 also forms multiple disulfides with unknown target proteins during H_2O_2 treatment, the formation of which is also potentiated in cells expressing the C53A mutant. This suggests that the intersubunit disulfide induces a conformational change that limits Cys-106 forming heterodisulfide protein complexes or from hyperoxidizing. High concentrations of H_2O_2 also induce cell death, with DJ-1 Cys-106 sulfonation appearing causal in these events, as expression of C53A DJ-1 enhanced both Cys-106 sulfonation and cell death. Nonetheless, expression of the DJ-1 C106A mutant, which fully prevents hyperoxidation, also showed exacerbated cell death responses to H_2O_2. A rational explanation for these findings is that DJ-1 Cys-106 forms disulfides with target proteins to limit oxidant-induced cell death. However, when Cys-106 is hyperoxidized, formation of these potentially protective heterodimeric disulfide complexes is limited, and so cell death is exacerbated.

Oxidative stress is associated with a net increase in concentration of reactive oxygen species and is implicated in the pathogenesis of heart disease, including ischemia/reperfusion injury, cardiac hypertrophy, and heart failure. Reactive oxygen species may be injurious by causing oxidative damage or dysregulating homeostatic redox signaling pathways. Antioxidant reactive oxygen species-neutralizing defense mechanisms maintain the cellular environment in a reduced condition, limiting oxidation of proteins and other biomolecules. Parkinson protein 7 (DJ-1) is one of the most abundant redox-sensitive proteins within the heart. However, little is known about its response during cardiac oxidative stress.

Human DJ-1 contains 189 amino acid residues and exists as a homodimer of two ~20-kDa subunits (1). DJ-1 was first identified as an oncogene (2) and has since been described as a causative gene for early-onset Parkinson disease (3, 4). Although DJ-1 has protease (5–7) or chaperone (8, 9) activities, most studies have focused on its protective role against oxidative stress (10–15). Knock-out of the DJ-1 gene enhances hydrogen peroxide (H_2O_2) and 1-methyl-4-phenyl-1,2,3,6-tetrahydropyridine-mediated cell death. Furthermore, examination of mitochondria from KO mice revealed that DJ-1 acts as an atypical peroxiredoxin-like peroxidase that has the ability to scavenge H_2O_2 (16). DJ-1 can also bind to mRNA encoding factors such as protein 53 (p53) (20) and proteins involved in glutathione synthesis (17), but when oxidized it releases these factors to facilitate translation of oxidative stress response proteins. For all these reasons DJ-1 is generally considered to be an antioxidant protein.

The cysteine residues in this protein are crucial for its cytoprotective activity (18, 19). Human DJ-1 contains three cysteine residues, Cys-46, Cys-53, and Cys-106. Cys-106 is the most conserved cysteine and is a critical mediator of many of DJ-1 functions (20). The Cys-106 thiol residue has an acid dissociation constant (pK_a) of 5.4 (21), meaning it is predominantly ionized at physiological pH, explaining its reactivity with oxidants (16, 22). Cysteine residues can be oxidized to three distinct species by the cumulative additions of oxygen, successively forming cysteine-sulfenic (-SOH), -sulfinic ($-SO_2H$), and -sulfonic ($-SO_3H$) acid. These three species have different physicochemical characteristics. Peroxide-induced formation of a disulfide bond between two cysteine thiols is generally mediated by sulfenic acid formation or by thiol-disulfide exchange (23). Such post-translational oxidative modifications may lead to perturbations in conformation, stability, molecular interactions, or activity of proteins such as DJ-1, providing a potential mechanism of their redox regulation.

Mammalian peroxiredoxins (Prdx)[2] proteins are peroxidases composed of three main groups according to the number of

* This work was supported by the European Research Council (ERC Advanced award), British Heart Foundation, Medical Research Council and Fondation Leducq, and the Department of Health via the National Institute for Health Research (NIHR) Comprehensive Biomedical Research Centre award to Guy's and St. Thomas' National Health Service Foundation Trust. The authors declare that they have no conflicts of interest with the contents of this article.

[S] This article contains supplemental Table S1 and Fig. S1 and S2.

[1] To whom correspondence should be addressed. Tel.: 44-20-7188-0969; Fax: 44-20-7188-0970; E-mail: philip.eaton@kcl.ac.uk.

[2] The abbreviations used are: Prdx, peroxiredoxin; Trx, thioredoxin; PLA, proximity ligation assay; MTT, 3-(4,5-dimethylthiazol-2-yl)-2,5-diphenyltetrazolium bromide.

active cysteines and their positional variation, including the typical 2-Cys Prdxs, the atypical 2-Cys Prdxs, and the 1-Cys Prdxs (24, 25). Dimeric Prdx1, Prdx2, Prdx3, and Prdx4 are typical 2-Cys Prdxs in which the peroxidatic thiol reacts with H_2O_2 to form a sulfenic acid, which is then "attacked" by a resolving cysteine on the other monomer in the functional pair. The resulting Prdx disulfide dimer is reduced by the disulfide reductase thioredoxin (Trx) to regenerate reduced Prdx proteins capable of decomposing another molecule of H_2O_2 (26). When the Trx reduces the oxidized Prdx, it does so at the expense of becoming oxidized itself via a thiol disulfide-exchange reaction. Prdx may also thiol-disulfide exchange with other proteins and induce disulfide bond formation, thereby potentially modifying their activities. For example, Prxd4 directly oxidizes protein disulfide isomerase within the endoplasmic reticulum, thereby increasing the oxidative folding of substrates such as RNase A (27). Similarly, Prdx2 (~22 kDa) attenuates the transcriptional activity of STAT3 likewise through disulfide-bond formation (28). In this way Prdx serves as a sensor that "picks up" increases in a cellular oxidant signal by virtue of disulfide bond formation. This signal can then transduced by the aforementioned thiol-disulfide exchange reaction to induce oxidation of a target protein whose activity may be redox-state dependent. In this way proteins that may not directly react with oxidants may still become oxidized but, indirectly, with Prdx oxidation serving as an intermediate step.

The redox state of DJ-1 in HEK cells, isolated cardiomyocytes, or isolated hearts exposed to increasing concentrations of H_2O_2 was shown to undergo complex redox state changes. Transfection studies with C53A or C106A DJ-1 mutants show the oxidation state of either of these individual cysteines impacts on the susceptibility of the other to oxidation, with interventions that promote hyperoxidation of Cys-106 exacerbating H_2O_2-induced cell death. H_2O_2-induced DJ-1 disulfide formation was found to occur via a mechanism in which Prdx2 first reacts with the oxidant to form a disulfide, which is then transmitted to DJ-1, likely via a thiol-disulfide exchange reaction.

Experimental Procedures

This investigation was performed in accordance with the Home Office Guidance on the Operation of the Animals (Scientific Procedures) Act 1986, published by Her Majesty's Stationery Office (London, UK). Animals were maintained humanely in compliance with the "Principles of Laboratory Animal Care" formulated by the National Society for Medical Research and the Guide for Care and Use of Laboratory Animals prepared by the National Academy of Sciences and published by the National Institutes of Health (NIH publication no. 85-23, revised 1985). All animal protocols were approved both by the local King's College Ethical Review Process Committee and by the UK Government Home Office (Animals Scientific Procedures Group).

Studying DJ-1 Oxidation in Isolated Rat Cardiomyocytes or Hearts Perfused with H_2O_2—Ventricular myocytes were isolated from hearts of male Wistar rats (body weight, 200–250 g) as described previously (29). In brief, the rats were anesthetized with pentobarbitone sodium (40 mg intraperitoneally) and injected with sodium heparin (200 IU) via the femoral vein. Hearts were excised and perfused for 5 min with modified HEPES-Krebs solution (pH 7.3 at 37 °C) containing 0.75 mmol/liter $CaCl_2$. Then, hearts were consecutively perfused with Ca^{2+}-free HEPES-Krebs solution containing 100 μmol/liter EGTA (4–10 min) and with HEPES-Krebs solution containing 100 mmol/liter $CaCl_2$ and 1 mg/ml type II collagenase (Worthington) (8 min). Subsequently the ventricles were removed and cut into small pieces. Single cells were separated from undigested ventricular tissue by filtering through nylon gauze and stored in the taurine-containing solution until the myocytes settled down. The isolated myocytes were cultured in pre-laminated 6-well culture plates or on individual 3.5-cm dishes for confocal microscopy with modified M199 culture medium (Invitrogen) containing 2 mmol/liter creatine, 2 mmol/liter carnitine, and 5 mmol/liter taurine plus 100 IU/ml penicillin/streptomycin. The culture medium was replaced after 2 h, and the cells were maintained overnight. The next day cardiomyocytes were treated with H_2O_2 (0–200 μM) for 10 min or with auranofin (1–3 μg, Sigma).

Rat hearts were also isolated, cannulated, and perfused in Langendorff mode at a constant flow of 12 ml/min as follows: 30 min of aerobic perfusion with bicarbonate buffer followed by 5 min of perfusion with 0–500 μM H_2O_2 in bicarbonate buffer. At the end of the perfusion protocol, hearts were frozen and stored in liquid nitrogen until further analysis. Hearts were homogenized using a tissue grinder (Polytron) in cold buffer containing 100 mM Tris-HCl, pH 7.2, 100 mM maleimide, and protease inhibitors (Complete C, Roche Applied Science).

In Vitro Preparation of WT and DJ-1 Cysteine Mutants and Prdx2—HEK 293T cells were maintained in DMEM supplemented with 10% FBS and transfected using Lipofectamine 2000 (Invitrogen) according to the manufacturer's instructions. The mammalian expression plasmids for DJ-1 WT and mutants were acquired from Addgene (DJ-1 WT plasmid #29416, DJ-1 C53A plasmid #29419 and DJ-1 C106A plasmid #29409). The Prdx2 plasmid (#31338, Addgene) was subcloned into a mammalian expression vector using a pcDNA™ 3.3-TOPO® TA Cloning® kit (Invitrogen). Two days after transfection cells were treated with H_2O_2 (0–500 μM) for 10 min.

Immunoblotting Analysis and Immunoprecipitation of DJ-1—Protein samples prepared from hearts, and cardiomyocytes were loaded (200 μg) and separated by SDS-PAGE using the Mini Protean 3 system (Bio-Rad) and transferred to PDVF membranes (GE Healthcare). Blots were incubated with the following primary antibodies diluted 1:000 in PBS-Tween 5% milk overnight: DJ-1 (ab18257, Abcam), V5-tag (ab27671, Abcam), Prdx2 (ab15572, Abcam), and a SO_3H-Cys-106 DJ-1 antibody generated in-house as detailed below. One hour of incubation with horseradish peroxidase-coupled anti-mouse (#7076, Cell Signaling) and anti-rabbit (#7074, Cell Signaling) IgG secondary antibody (diluted 1:1000 in PBS-Tween 5% milk) was used to detect primary antibodies bound to the blot together with enhanced chemiluminescence reagent (GE Healthcare).

Cardiomyocytes were lysed in radioimmune precipitation assay buffer (10 mM Tris, pH 7.4, 140 mM NaCl, 0.1% Triton X-100 0.1% SDS, and 1% sodium deoxycholate) supplemented

with protease inhibitor mixture (Complete C, Roche Applied Science). The lysates were then incubated with DJ-1 antibody (ab18257, Abcam) overnight on a rotating wheel. The next day A/G-agarose beads (sc-2003, Santa Cruz) were added to the samples according to the manufacturer instructions. After 3 washes with radioimmune precipitation assay buffer the precipitates were resuspended in Laemmli sample buffer containing 5% β-mercaptoethanol at 95 °C. To precipitate DJ-1 WT and cysteine mutants, HEK 293T cells were lysed in radioimmune precipitation assay buffer, incubated with V5-beads (A7345, Sigma) overnight, and washed three times with radioimmune precipitation assay buffer. Finally, precipitates were resuspended in Laemmli sample buffer containing 5% β-mercaptoethanol.

Proteomic Analysis—20 μg of protein obtained from DJ-1 immunoprecipitated from cardiomyocytes were loaded and separated on 4–12% polyacrylamide gradient gels (NuPAGE, Bio-Rad). After electrophoresis, gels were silver-stained, and a 75-kDa band was excised and subjected to in-gel digestion with molecular grade trypsin (ThermoScientific) using standard protocols. Tryptic peptides were separated on a nanoflow LC system (Dionex UltiMate 3000) and eluted with a 40-min, 4-step gradient (10–25% B in 35 min, 25–40% B in 5 min, 90% B in 10 min, and 2% B in 30 min, where A was 2% acetonitrile (ACN), 0.1% formic acid in HPLC H_2O, and B was 90% ACN, 0.1% formic acid in HPLC H_2O). The column (Dionex PepMap C18, 25-cm length, 75-μm internal diameter, 3-μm particle size) was coupled to a nanospray source (Picoview) using RePlay (Advion) to obtain a technical duplicate of the LC-MS/MS. Spectra were collected from an ion trap mass analyzer (LTQ-Orbitrap XL, ThermoFisher Scientific). MS/MS peak lists were generated by extract_msn.exe and matched to a rat database (UniProtKB/Swiss-Prot, 35702 protein entries) using SEQUEST and X! Tandem. Peptide identifications were accepted if they could be established at >95.0% probability as specified by the Peptide Prophet algorithm 3. Protein identifications were accepted if they could be established at >99.0% probability with at least two independent peptides.

DJ-1 Cys-106-SO_3H Detection by Immunoblotting—The active site peptide KGLIAAIC*AGPT was synthesized with sulfonic acid (cysteic acid) incorporated in place of the catalytic Cys-106 (C*) (PARK7_RAT) and coupled to KLH, and the rabbits were immunized. IgGs selective against DJ-1 sulfonylated at Cys-106 were purified by affinity capture using a hyperoxidized peptide attached to a column. IgGs were eluted with sequential low and high pH washes, and the antibody described resided in the low pH elution pool.

Immunofluorescence and Proximity Ligation Assay (PLA) Analysis—Cardiomyocytes and HEK 293 cells were fixed with 4% paraformaldehyde (Sigma) in PBS for 10 min at room temperature, washed in PBS, and permeabilized with 0.2% Triton X-100 in PBS for 5 min. To avoid nonspecific antibody binding, the cells were incubated with blocking buffer (5% nonspecific goat serum diluted in 1% bovine serum albumin, Tris-base 20 mmol/liter, NaCl 155 mmol/liter, EGTA 2 mmol/liter, $MgCl_2$ 2 mmol/liter, pH 7.5) for 1 h at room temperature. Cells were incubated in primary antibody diluted (1:100) in blocking buffer overnight at 4 °C and washed with PBS the next day. For double immunofluorescence with V5-tag (ab27671, Abcam) and SO_3H-Cys-106 DJ-1 antibodies, a combination of Cy3-conjugated anti-rabbit (111-165-144, Jackson ImmunoResearch) and Cy5-conjugated anti-mouse (115-177-003, Jackson ImmunoResearch) secondary antibodies were used at a 1:100 dilution for 1 h at room temperature. Diamidine-2-phenylindole dihydrochloride (D8417, Sigma) was added with the secondary antibodies to stain the nucleus.

The *in situ* PLA experiments were performed using the Duolink® In Situ Red Starter Kit Mouse/Rabbit (DUO92101, Sigma) according to the manufacturer's instructions. Samples were mounted in Lisbeth's medium onto microscope slides and were analyzed using confocal microscopy on an inverted microscope (Leica SP5 system) equipped with a blue diode and argon and helium neon lasers. For PLA analysis of HEK 293 T cells V5 tag (ab27671, Abcam) and His tag (#12698, Cell Signaling) primary antibodies were uses at 1:100 dilutions.

Analysis of Cell Death by 3-(4,5-Dimethylthiazol-2-yl)-2,5-diphenyltetrazolium Bromide (MTT) Assay and Apoptosis by Flow Cytometry in DJ-1 WT and Cysteine Mutants—A total of 7×10^6 HEK293 cells plated in 6-well flat-bottom plates were treated with 200 μM H_2O_2 for 18 h. At the indicated times, the cells were incubated for 30 min with 0.5 mg/ml dye MTT and then with 500 μl of stop solution (0.1 N HCl, 10% Triton X-100 in isopropyl alcohol) was added to each well to dissolve the formazan crystals. The absorbance at 570 nm was determined using a Gemini XPS plate reader (Molecular Devices). Triplicate wells were assayed for each condition.

For the flow cytometry protocol transfected cells were harvested, washed with PBS, and incubated for 30 min with 1 μl of the reconstituted live/dead cell stain (#L34957, Life Technologies). After the incubation time HEK293 cells were washed with PBS and incubated for 20 min with annexin V-APC antibody (#A35111, Life Technologies) diluted in annexin binding buffer (#V-13246, Life Technologies) following the manufacturer's instructions. HEK 293 cells were washed with annexin binding buffer and resuspended in 500 μl of fixation/permeabilization buffer (#GAS003, Life Technologies) for 20 min. The fixation buffer was removed by washing the cells with Perm/Wash buffer (#GAS003, Life Technologies). Finally, the cells were incubated with V5-tag FITC (#R96325, Life Technologies) and cleaved caspase-3 (Asp-175) (#12768S, Cell Signaling) for 30 min and washed with FACS (PBS, 2% BSA). The suspension was analyzed on a FACS Canto (BD Biosciences). Data were analyzed with FlowJo version 7.6.5 (Treestar, Inc.). The median fluorescence intensities were calculated on an arbitrary scale.

Statistical Analysis—The effect of H_2O_2 on the different DJ-1 mutants was analyzed by one- or two-way analysis of variance followed by Bonferroni post-hoc test using GraphPad Prizm 4 software. Normality was assessed by the Shapiro-Wilk test, and homogeneity was assessed by a residual plot. Differences were considered significant at $p < 0.05$.

Results

Oxidant-induced DJ-1 Redox State Alterations in Cardiomyocytes and Heart—Adult rat ventricular cardiomyocytes or isolated rat hearts were exposed to 0–200 or 0–500 μM H_2O_2, respectively. The cells or hearts were collected in buffer

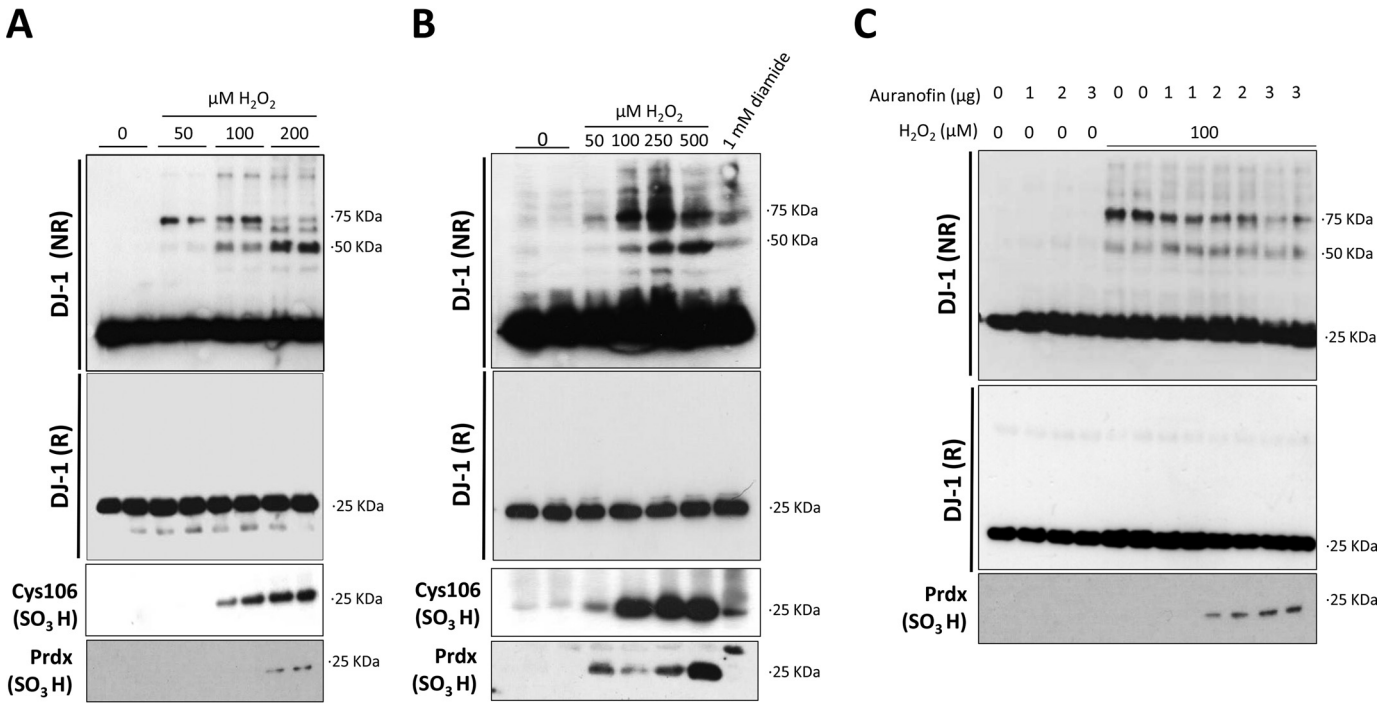

FIGURE 1. **Effect of H_2O_2 on the redox state of cardiac DJ-1.** Non-reducing immunoblots of cardiomyocytes or rat heart were probed with anti-DJ-1, anti-DJ-1 Cys-106SO_3H or 2 Cys PrdxSO_3 antibodies under reducing (R) or non-reducing (NR) conditions. *A*, cardiomyocytes were treated with 0–200 μM H_2O_2 for 10 min. *B*, rat hearts were perfused with 0–500 μM H_2O_2 or 1 mM diamide. *C*, cardiomyocytes were treated for 30 min with 1–3 μg of auranofin followed by treatment with 100 μM H_2O_2 for 10 min.

with maleimide, an alkylating agent that limits any further oxidation of cysteinyl thiols. Immunoblotting analysis of cardiomyocytes (Fig. 1*A*) or hearts (Fig. 1*B*) showed that DJ-1 migrates as a monomer under basal non-reducing conditions. However, H_2O_2 treatment induced formation of DJ-1 disulfide species, which were absent when electrophoresis was performed under reducing conditions. This oxidant-induced disulfide formation occurred robustly both in cardiomyocytes (supplemental Fig. S1*A*) and in heart (supplemental Fig. S1*B*), showing a consistent banding pattern. The lower concentrations of H_2O_2 induced a 75-kDa disulfide complex that was lost when higher levels were used, at which point a 50-kDa disulfide complex appeared. The 50-kDa band was likely to correspond to a DJ-1 disulfide dimer, consistent with conjugation of two ~25-kDa DJ-1 monomers, which are known to be proximal to each other. H_2O_2 at 100–500 μM was sufficient to oxidize Cys-106 in cardiomyocytes (Fig. 1*A*) or hearts (Fig. 1*B*) to the sulfinic or sulfonic acid state, termed hyperoxidation. To assess the formation of these disulfide complexes in the myocardium, isolated hearts were also perfused with 1 mM diamide. Diamide also promoted the 50- and 75-kDa DJ-1 disulfide complexes (Fig. 1*B*) but less efficiently than that achieved by H_2O_2.

To establish whether the redox state of DJ-1 can be regulated by the Trx system, cardiomyocytes were pretreated with auranofin before inducing DJ-1 oxidation. Auranofin is an inhibitor of selenocysteine enzymes including thioredoxin reductase. Co-treatment with auranofin limited the amount of H_2O_2-induced 75 kDa complex and promoted the formation of the 50-kDa disulfide dimer (Fig. 1*C*).

Interaction of DJ-1 with Prdx2—Proteins that potentially form disulfide interactions with DJ-1 after oxidant interventions to mediate the 75-kDa complex were identified (Table 1). This was achieved by immunoprecipitating DJ-1 from vehicle or H_2O_2-treated cardiomyocytes, resolving the sample by SDS-PAGE, excising a 75-kDa gel band piece from each sample lane, and analyzing each of them for constituent proteins using mass spectrometry. Consistent with mass spectrometry being very sensitive, several proteins were identified in the two samples despite the immunoprecipitation step (supplemental Table S1). As expected, these included proteins with a mass of ~75 kDa, but smaller proteins such as glyceraldehyde-3-phosphate dehydrogenase, myoglobin, and triosephosphate isomerase were enriched in the samples from cells exposed to H_2O_2. These, perhaps unexpected, smaller proteins may be present as they also form disulfide complexes in response to oxidant treatment of cardiac myocytes (30). Prdx1 and Prdx2 were also identified as potential DJ-1 binding partners in response to H_2O_2 treatment. However, when we performed detailed followup analysis of the disulfide interaction of DJ-1 with these Prdx isoforms (see below) no independent corroboration of an interaction with Prdx1 could be found. Thus the primary focus of this study was on Prdx2, and its oxidant-induced complexation with DJ-1 (Fig. 2). The efficiency of the IP was checked by running the soluble cell lysate, labeled *Input* on Fig. 3*A*, together with the immunoprecipitated material on the same gel. Silver staining the gel highlighted a ~25-kDa band, corresponding with the molecular mass of the DJ-1 monomer, present in the IP samples (Fig. 3*A*). This putative enrichment of DJ-1 in the immunoprecipitate was subsequently validated by Western blot (Fig. 3*B*).

TABLE 1
Proteins identified in 75-kDa gel bands after immunoprecipitation of DJ-1 from control or H_2O_2-treated rat ventricular cardiomyocytes

Identified proteins	Accession number	Molecular mass	*p* value	Quantitative value[a]					
				50 μM H_2O_2			Controls		
		kDa		10^4			10^4		
Peroxiredoxin-1	Q63716	22	0.004	9.26	5.54	10.08	0	0	0
Peroxiredoxin-2	P35704	22	0.050	7.04	4.34	1.62	0	0	0
Triosephosphate isomerase	P48500	27	0.030	3.23	8.85	11.09	0	0	0
Glyceraldehyde-3-phosphate dehydrogenase	E9PTN6	36	0.002	16.99	10.46	17.08	0	0	0
Fructose-bisphosphate aldolase	G3V900	45	0.000	5.34	4.21	5.73	0	0	0
Myoglobin	Q9QZ76	17	0.023	9.76	10.67	3.91	0.33	0.87	0.34
E3 ubiquitin-protein ligase	Q6AXU4	19	0.000	0	0	0	2.87	2.73	2.26
Phosphoglucomutase 1	Q499Q4	61	0.046	195.54	230.89	192.33	154.50	177.57	132.26
Acyl-coenzyme A dehydrogenase, very long chain	Q5M9H2	71	0.003	159.97	162.13	152.58	242.11	293.71	298.27
EH-domain containing 4	Q8R3Z7	61	0.015	88.36	76.68	79.70	63.60	51.27	42.29
Dihydrolipoyllysine-residue acetyltransferase component of pyruvate dehydrogenase complex	P08461	67	0.002	42.64	27.64	26.36	74.98	88.90	76.30
Carnitine *O*-palmitoyltransferase 2	P18886	74	0.035	58.55	52.97	65.49	79.91	84.58	111.53
Acyl-CoA synthetase family member 2	Q499N5	68	0.037	54.09	43.71	56.45	65.04	76.83	64.33
RCG37494	D3ZZN3	75	0.017	26.66	23.20	19.13	44.18	55.85	73.72
Rab GDP dissociation inhibitor α	P50398	51	0.004	24.93	29.89	36.33	12.24	7.10	63.03
Protein kinase, AMP-activated, α2 catalytic subunit	G3V715	62	0.021	0	3.41	1.28	16.05	8.83	87.02
RCG23609, isoform CRA	G3V885	224	0.032	120.80	103.28	157.28	68.48	47.30	82.06
Phosphorylase	G3V8V3	97	0.049	4.10	2.01	4.30	0	2.03	0

[a] The quantitative value is a normalized value that takes into account the sum of the "unweighted spectrum counts" for each sample analyzed by mass spectrometry. The scaling factor for each immunoprecipitated sample was applied to each protein group and adjusted its "unweighted spectrum count" to a normalized "quantitative value." Statistical significance was calculated using a *t* test. Please refer to supplemental Table S1 and Fig. S1 and S2.

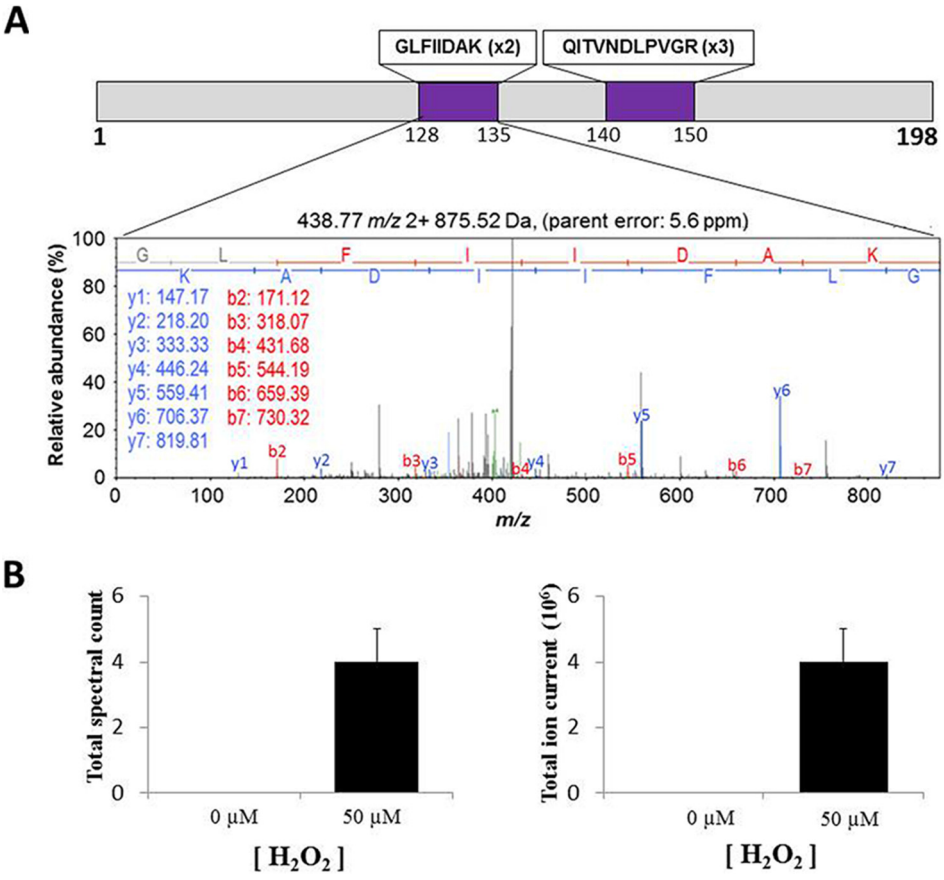

FIGURE 2. *A*, annotated MS/MS spectra for peptide GLFIIDAK of rat Prdx2 detected after immunoprecipitation of DJ-1 from cardiomyocytes treated with 50 μM H_2O_2. The GLFIIDAK and QITVNDLPVGR peptides were detected two (*x*2) and three times (×3), respectively. *B*, Prdx2 total spectrum count and total ion current for each sample from three independent cardiomyocyte isolations under control conditions or exposure to 50 μM H_2O_2.

Prdx2 was also detected in the DJ-1 immunoprecipitated samples from cardiomyocytes, but there was more co-capture of the Prdx when cells had been exposed to H_2O_2. Proximity ligation assay analysis corroborated the results obtained by Western immunoblotting, showing that DJ-1 and Prdx co-localize *in situ* in cardiomyocytes after exposure to H_2O_2 (Fig. 3*C*).

Potentiated Interprotein Disulfide Bond Formation and Cys-106 Hyperoxidation in C53A DJ-1—To determine whether the redox state of a thiol in DJ-1 impacted on the susceptibility of others to oxidation, the responses of C53A or C106A DJ-1 "redox dead" mutants in response to H_2O_2 were examined. WT, C53A, and C106A DJ-1 was expressed in HEK cells,

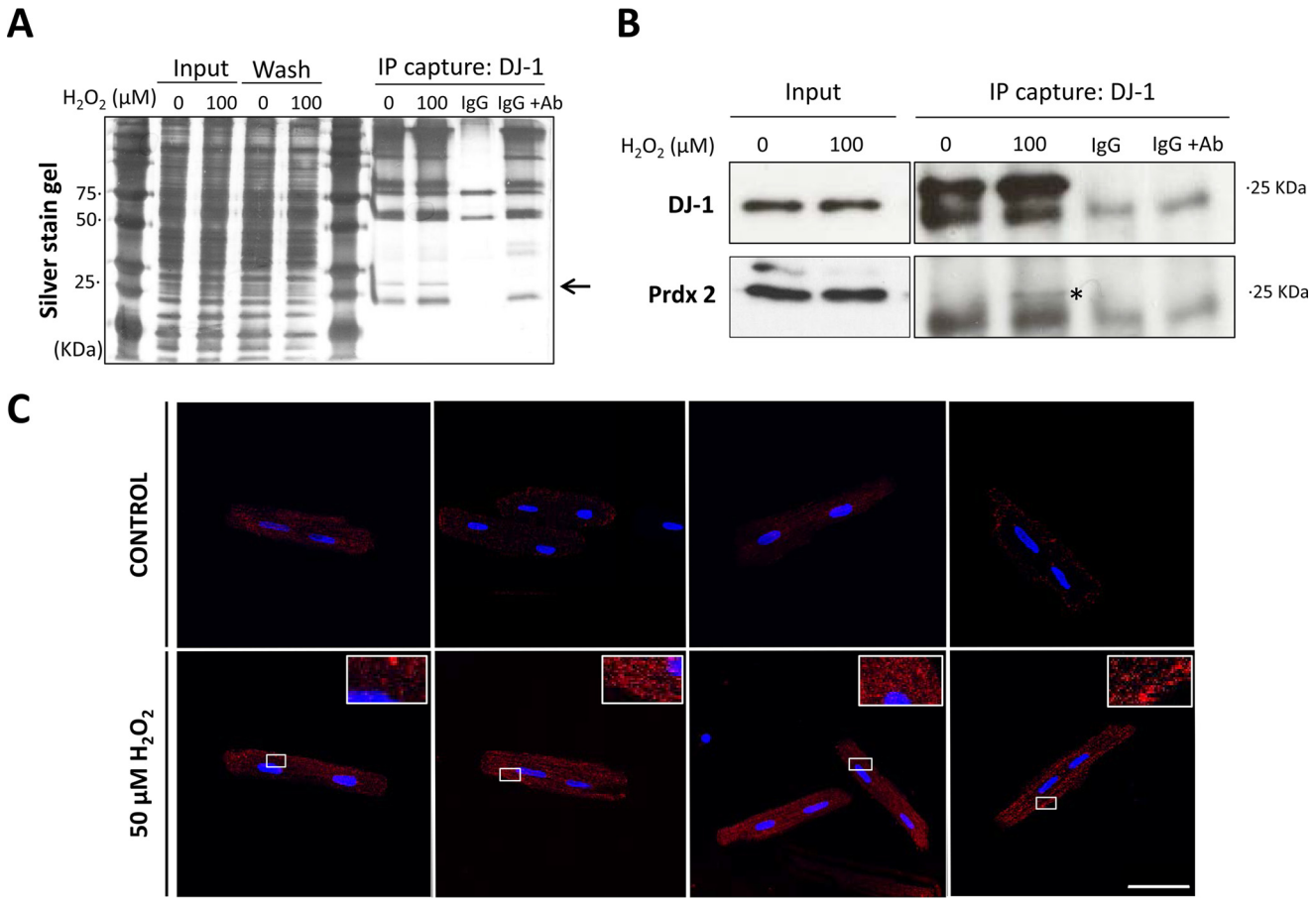

FIGURE 3. **Oxidative stress promoted interaction of DJ-1 with Prdx2.** *A*, silver-stained gel of DJ-1 immunoprecipitated (*IP*) from cardiomyocytes. *B*, immunoblot showing Prdx2 co-immunoprecipitation with DJ-1. Cardiomyocytes were treated with or without 100 μM H_2O_2, after which cell lysates were prepared, and DJ-1 was immunoprecipitated and analyzed by immunoblotting with an antibody to Prdx2 or DJ-1. The Prdx2 band is highlighted (*). IgG corresponds to agarose IgG beads, and IgG+Ab corresponds to IgG beads and DJ-1 antibody. *C*, representative image from a proximity ligation assay, which allows possible protein-protein interactions between DJ-1 and Prdx2 to be assessed. Cardiomyocytes were treated with 0 or 50 μM H_2O_2 for 10 min and then stained with antibodies to DJ-1 and Prdx2. The nucleus was stained *blue* with b4′,6-diamidino-2-phenylindole (DAPI). Each *red dot* represents the detection of protein-protein complexes between DJ-1 and Prdx2, which are markedly increased after H_2O_2 treatment. *Scale bar*: 50 μm.

which were then treated with H_2O_2. WT or C53A, but not the C106A mutant, formed an array of disulfide bonds with target proteins after H_2O_2 treatment (Fig. 4*A*). Surprisingly, the C53A mutant showed potentiated levels of interprotein disulfide bond formation with target proteins after H_2O_2 treatment compared with WT. This exacerbated response of the C53A DJ-1 mutant to H_2O_2 was especially apparent when it was immunoprecipitated via its V5-tag beads, resolved on a gel, and silver-stained. It was evident that a large number of proteins co-purified with C53A DJ-1 after cells were exposed to H_2O_2 (Fig. 4*B*).

The C53A mutant is also more susceptible to Cys-106 oxidation compared with the WT, consistent with the possibility that the disulfide bond between the two DJ-1 monomers may protect Cys-106 from hyperoxidation (Fig. 4*A*). Double immunofluorescence studies using antibodies to the V5 tag on transfected DJ-1 or to that which hyperoxidized (SO_3H-Cys-106) further corroborated the findings based on co-immunoprecipitation. Thus, SO_3-Cys-106 immunolabeling was only observed in HEK 293 cells treated with H_2O_2 if they were transfected with C53A DJ-1 mutant (Fig. 4*C*). Because the Cys-106 is the most reactive cysteine, the band pattern observed with the C53A mutant may correspond with disulfide bonds between the Cys-106 and target proteins.

DJ-1 Cys-53 Is Needed for Its Interaction with Prdx2—To determine which of the DJ-1 cysteines is required for the interprotein disulfide linkage with the Prdx, HEK 293 cells were transfected with plasmids for WT, C53A, or C106A together with Prdx2 and then treated with 0 or 100 μM H_2O_2. DJ-1 protein was immunoprecipitated using V5 beads, and the interaction with Prdx2 was checked by Western blot analysis to assess co-purification. Prdx2 interacted with both WT and C106A DJ-1, but not the C53A variant, implying that Cys-53 is critical for disulfide bond formation between both proteins (Fig. 5*A*). Although the Prdx2/DJ-1 WT and Prdx2/DJ-1 C106A interactions were detected in both treated and untreated cells, it was markedly higher in those cells subjected to H_2O_2 treatment. This background level of interaction may be due to a basal oxidative stress of the HEK 293 cells subjected to transfection. PLA analysis also confirmed that C53A DJ-1 and Prdx2 do not co-localize (Fig. 5*B*). Negative controls were included as in supplemental Fig. S2.

DJ-1 C53A and C106A Mutants Are Vulnerable to Cell Death due to Apoptosis—We next evaluated the impact of DJ-1 redox state on the viability of cells subjected to H_2O_2

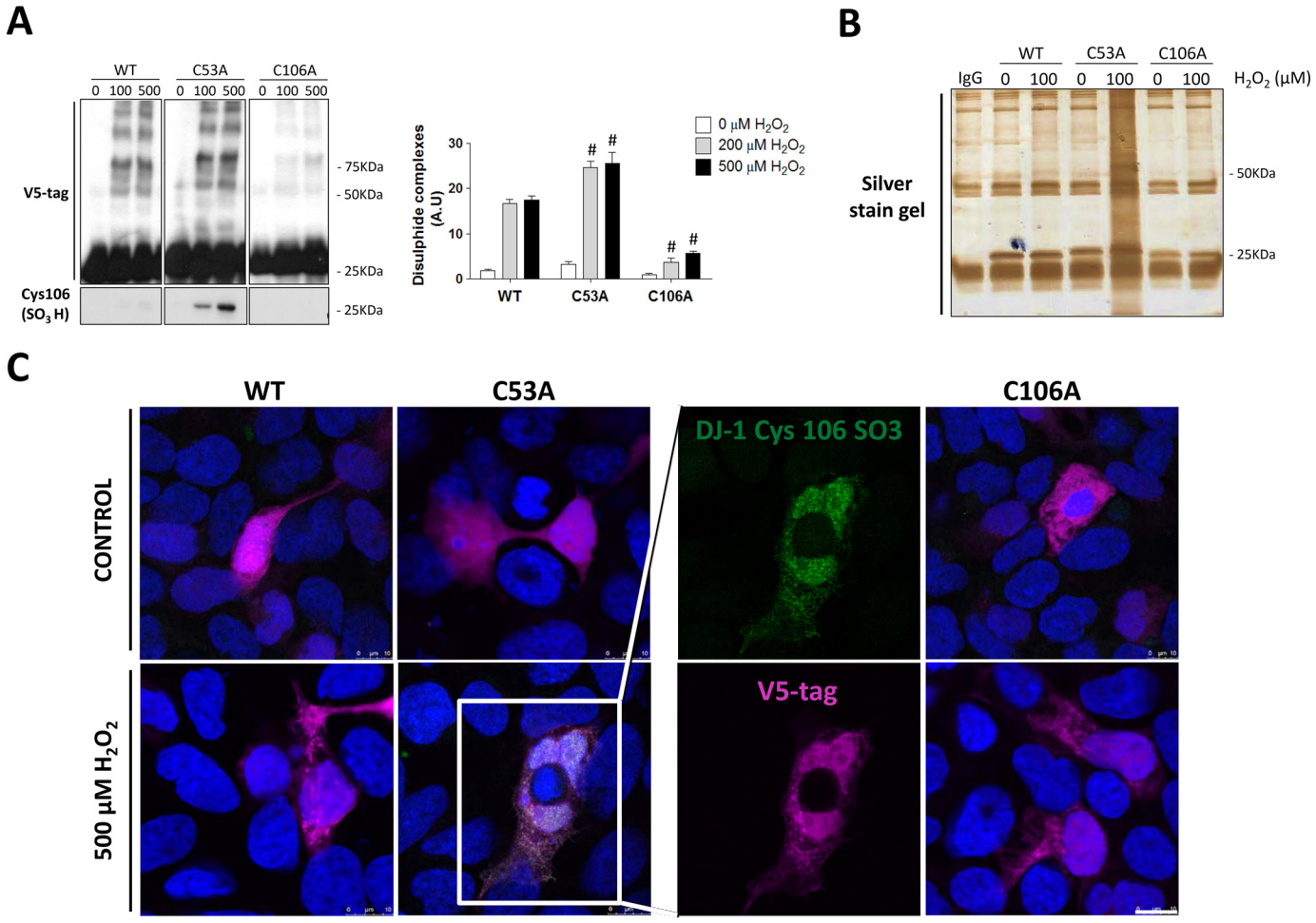

FIGURE 4. **C53A DJ-1 was more susceptible to H_2O_2-induced Cys-106 hyperoxidation than WT.** *A*, non-reducing immunoblots of HEK 293 cells lysates transfected with a WT, C53A, or C106A DJ-1 plasmid probed with antibodies to the V5 tag on the transfected DJ-1 or to hyperoxidized Cys-106SO_3H DJ-1. HEK 293 cells were treated with 0, 100, or 500 μM H_2O_2 for 10 min. The formation of disulfide-dependent complexes as well as Cys-106 hyperoxidation was significantly higher in the Cys-53 mutant. Cells transfected with C106A DJ-1 were less susceptible to disulfide complex formation compared with those cells transfected with the WT protein. Statistical significance was calculated using two-way analysis of variance with the Bonferroni post hoc test. #, $p < 0.001$. *B*, silver-stained gel of immunoprecipitated DJ-1 from transfected HEK 293 cells lysates. Mutant DJ-1 proteins (WT, C53A, and C106A) were precipitated using V5-agarose beads from HEK 293 cells treated with 100 μM H_2O_2 for 10 min. *C*, double immunofluorescence with V5 tag (*green*) and SO_3H-Cys-106 DJ-1 (*pink*) antibodies in HEK 293 cells transfected with WT, C53A, or C106A plasmids and treated with 0 or 500 μM H_2O_2 for 10 min. *Scale bar*: 10 μm.

treatment. HEK 293 cells were transfected with WT or cysteine mutant DJ-1 and subsequently treated with 200 μM H_2O_2 for 18 h. An MTT viability assay showed cells expressing C53A or C106A DJ-1 had significantly reduced viability compared with those transfected with WT protein (Fig. 6*A*). However, the C53A mutant was the only one that showed reduced viability compared with the WT when the cells were co-transfected with Prdx2 and then exposed to H_2O_2 (Fig. 6*A*). The MTT assay is not able to discriminate if the cell injury was caused by apoptosis or necrosis. Thus, to monitor the impact of the DJ-1 redox state on cell apoptotic responses to H_2O_2, annexin V or cleaved caspase 3 in the transfected (*i.e.* V5-positive) cells were monitored using flow cytometry. No differences in the expression of cleaved caspase 3 between mutant and wild type cells were detected (Fig. 6, *B* and *D*). Nevertheless, a significant increase in annexin V-positive cells in the Cys-53- and Cys-106-transfected cells was observed (Fig. 6, *C* and *D*).

Discussion

DJ-1 is a ubiquitous redox-responsive protein with multiple functions. The human DJ-1 (PARK7) gene is mutated in rare forms of recessively inherited Parkinsonism (4) and is, therefore, widely studied in the neurology field. However, in recent years alterations in DJ-1 have also been associated with multiple diseases such as amyotrophic lateral sclerosis (30), various cancers (31–33), and androgen receptor regulation (34). Surprisingly, considering the DJ-1 is highly expressed in the myocardium, relatively little is known about its role there. However, the hearts of DJ-1 knock-out mice are hypertrophic and susceptible to failure (35). This implies a protective role for DJ-1 in the myocardium, but the molecular basis of this remains unclear. Here we show that DJ-1 undergoes complex and dynamic redox-state changes in cardiomyocytes and cardiac tissue during different H_2O_2 treatments. This imbalance caused by excessive oxidative stress has a central role in the development of cardiomyopathies (34, 35).

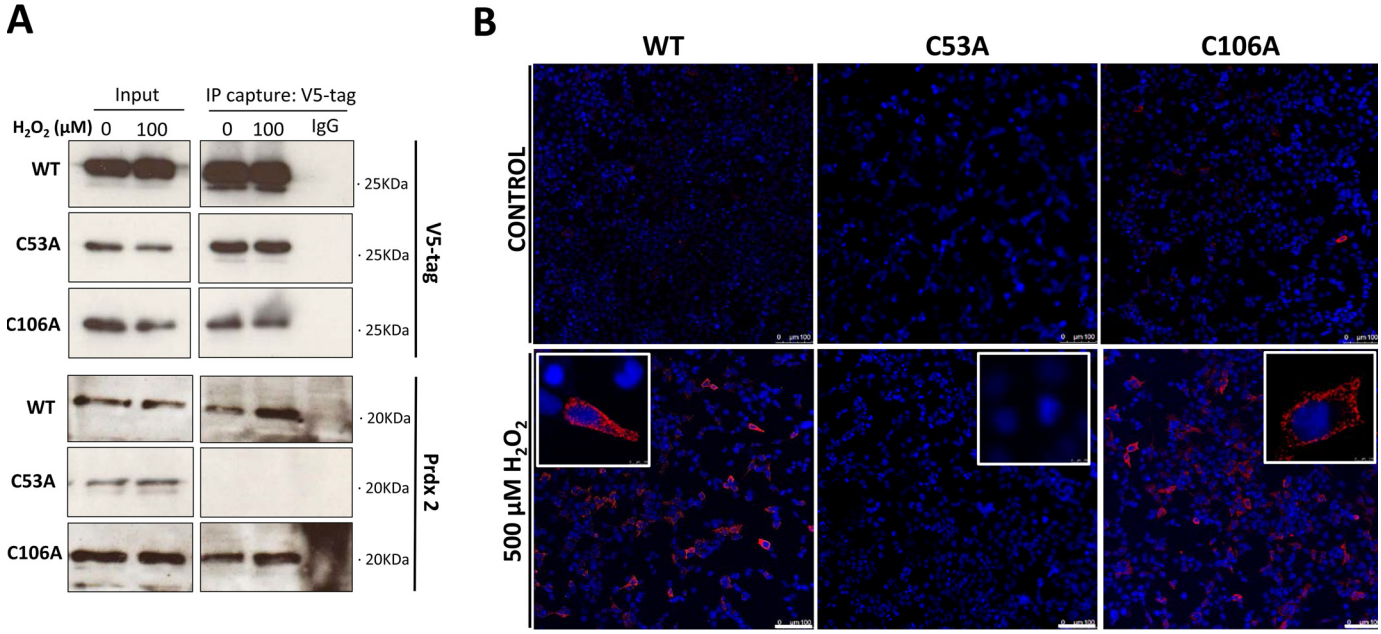

FIGURE 5. **Prdx2 interacted with DJ-1 Cys-53.** *A*, immunoblot showing Prdx2 co-immunoprecipitation (*IP*) with DJ-1. HEK 293 cells were transfected with WT, C53A, or C106A together with Prdx2 plasmids and then treated with 0 or 100 μM H_2O_2 for 10 min. Prdx2 co-precipitated with WT or C106A but not with the C53A DJ-1. *B*, representative image of proximity ligation assay assessing protein-protein interactions between DJ-1 mutants (WT, C53A, or C106A) and Prdx2. HEK 293 cells were treated with 0 or 500 μM H_2O_2 for 10 min and then stained with anti-V5 tag and His-tag antibodies. The nucleus was stained with b4′,6-diamidino-2-phenylindole (DAPI) nuclear staining (*blue*). Each *red dot* represents the detection of protein-protein complexes between DJ-1 and Prdx2. *Scale bar*: 100 μm.

In this study we observe sulfination or sulfonation of Cys-106 during high levels of peroxide, consistent with this thiol reacting with H_2O_2 to generate this hyperoxidized state. Cys-106 oxidation has already been proposed as a mechanism by which DJ-1 can act as a sacrificial oxidant scavenger (16). This irreversibly oxidized DJ-1 is subject to degradation, resulting in decreased expression (36). Billia *et al.* (35) reported low levels of DJ-1 protein in hearts from patients with heart failure, but their DJ-1 mRNA levels were not altered. Thus, based on our experiments, we suggest hyperoxidation of cardiac DJ-1 Cys-106 may serve as a posttranslational modification that triggers its degradation in patients with heart failure. We did not observe DJ-1 degradation, likely because cells were only exposed to an acute 10-min treatment with H_2O_2 in our study.

Previous studies have shown that Cys-106 is critical for multiple roles of DJ-1 and its interaction with target proteins (18, 37–39). Here we demonstrate that the redox state of Cys-53 is also important in controlling Cys-106 interdisulfide complex formation with target proteins. We observes a H_2O_2 dose-dependent increase of a 50-kDa complex that may correspond to the DJ-1 homodimer generated by disulfide bond formation between the Cys-53 from each monomer in cardiomyocytes or perfused hearts. Cys-53 is 3.3 Å from the equivalent residue on the adjacent subunit (1). Although relatively close, this is still too distant for a disulfide to bridge. However, we should also consider that the structure will have some flexibility and that the distance may change with interventions that modulate the oxidation of other cysteines in DJ-1 or upon binding of partner proteins.

It is also notable that the oxidant interventions only induce a relatively small proportion of the total pool of DJ-1 to the disulfide state. However, it is important to consider that such disulfides are readily reversible and can be continuously recycled back to the reduced state. Therefore, the Western blots may represent a snapshot of its redox cycle, not providing any information about the turnover rate of this process. Furthermore, DJ-1 interacts with many partners, potentially generating a variety of subcomplexes that may not all respond to oxidant in the same way, potentially delimiting the stoichiometry of disulfide formation.

A limitation of this study is an inability to differentiate between sulfinic and sulfonic hyperoxidation states of Cys-106 with the antibody used. Regardless of this, it is evident that a C53A DJ-1 mutant undergoes potentiated Cys-106 hyperoxidation. Intriguingly H_2O_2 treatment of cells expressing C53A DJ-1 also promoted formation of heterointerprotein disulfides with unidentified target proteins. During oxidative stress, the isoelectric point of DJ-1 changes from 6.2 to 5.8 (40), potentially explained by formation of the acidic hyperoxidation state well established to occur at Cys-106. However, a C53A DJ-1 was resistant to this oxidation-induced "acid shift" (19), which could be explained by Cys-53 hyperoxidation.

These observations are consistent with the interprotein disulfide between Cys-53 on DJ-1 subunits, which are found at the dimer interface (41), negatively regulating the susceptibility of Cys-106 to hyperoxidation. This Cys-53–Cys-53 homodisulfide dimer also serves to limit disulfide interactions of DJ-1 with other proteins. This leads to the rational suggestion that in the absence of a Cys-53–Cys-53 homodisulfide, Cys-106 has enhanced susceptibility to oxidation or disulfide formation with other proteins, perhaps because it becomes more accessible for such interactions. Such a rationale would explain why ASK1 (apoptosis signal-regulating kinase) was constitutively bound to C53A DJ-1 via Cys-106 (39). Structural changes induced by DJ-1 disulfide dimer formation may impact on the redox activity of Cys-106 and its capacity to form heterodisul-

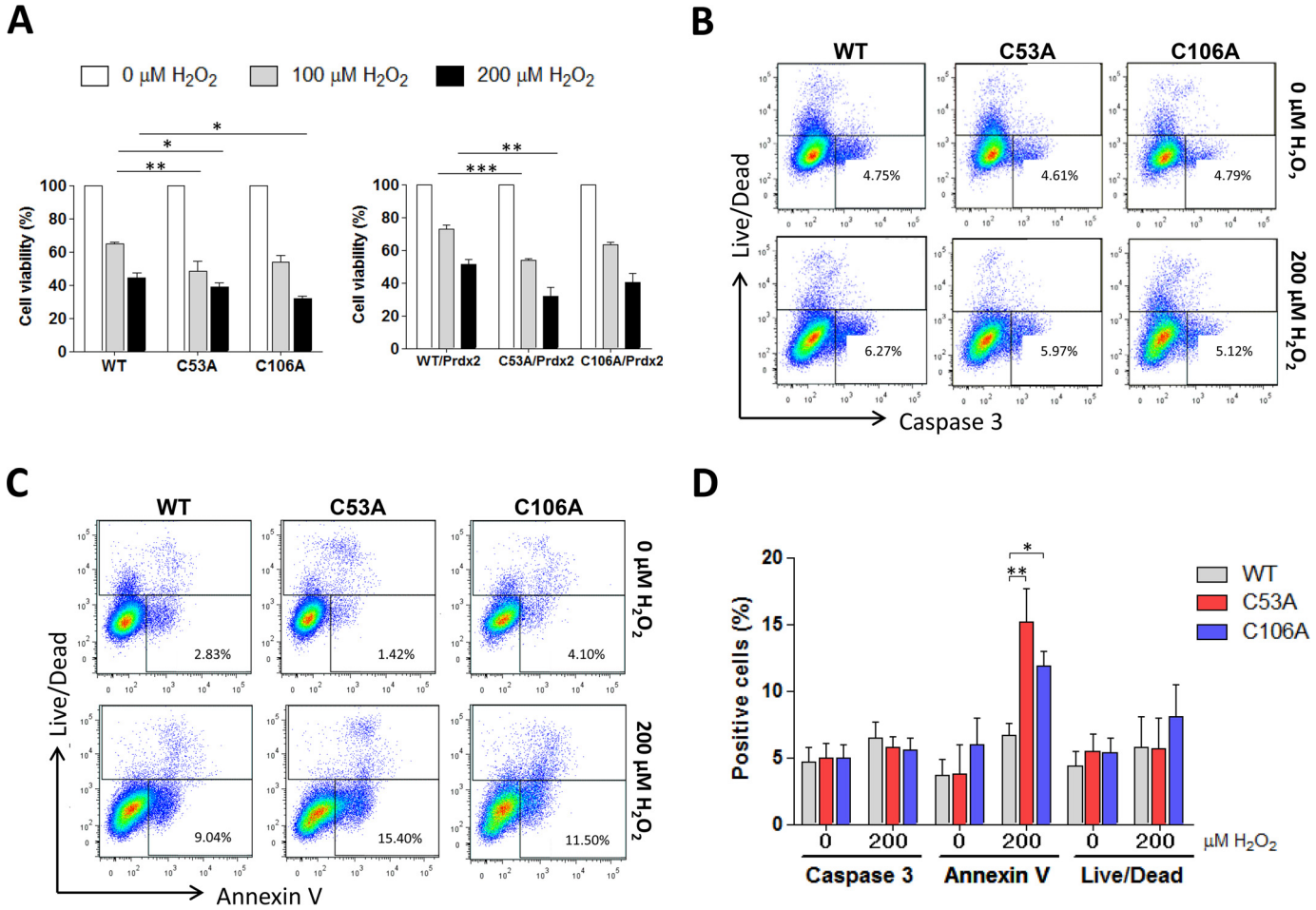

FIGURE 6. **Expression of C53A or C106A DJ-1 enhanced vulnerability to H_2O_2-induced apoptosis.** *A*, MTT assay of HEK 293 transfected with WT, C53A, or C106A DJ-1 plasmids alone or together with Prdx2. These cells were then treated with 0 or 200 μM H_2O_2 for 18 h. Statistical significance was calculated using two-way analysis of variance with Bonferroni post hoc test. *, $p < 0.05$; **, $p < 0.01$; ***, $p < 0.001$. *B* and *C*, representative flow cytometry results of cell apoptosis in HEK 293 cells (V5-positive) transfected with different DJ-1 constructs (WT, C53A, or C106A) using cleaved caspase 3 and annexin V antibodies. *D*, histograms represent the mean ± S.D. of the percentage of positive cells for cleaved caspase 3, annexin V, and live/dead-stained cells. HEK 293 cells were transfected with WT, C53A, or C106A plasmids and treated with 0 or 200 μM H_2O_2 for 18 h. Statistical significance was calculated using one-way analysis of variance with Bonferroni post hoc test. *, $p < 0.05$; **, $p < 0.01$; ***, $p < 0.001$.

fide protein complexes. DJ-1 Cys-106 forms disulfide bonds with multiple target proteins to limit oxidant-induced cell death (4, 14, 16, 42); thus when this residue hyperoxidizes it may lose its capacity to participate in this protective pathway. Our results showed that both Cys-106 and Cys-53 are important in the protective role of DJ-1 against apoptosis. Thus, the C106A mutant may promote injury because it cannot directly interact with proteins that otherwise may limit cell death, whereas the C53A mutant indirectly produces the same effect by promoting Cys-106 hyperoxidation.

One of the principal observations in this study was the formation of a 75-kDa DJ-1 complex before the appearance of the disulfide dimeric homodimer. Mass spectrometry analysis suggested this DJ-1 complex contained Prdx2, which was subsequently corroborated by co-immunoprecipitation studies as well as PLA analysis showing that DJ-1 Cys-53 was crucial for this interaction. Typical 2-Cys Prdx, such as Prdx2, have a peroxidatic cysteine with a very low pK_a, which in the presence of H_2O_2 is oxidized to a sulfenic acid and then attacked by a resolving cysteine located in other subunit. This reaction results in the formation of a stable intersubunit disulfide bond that is reduced by thioredoxin and constitutes a mechanism of degrading H_2O_2. The low pK_a of the peroxidatic cysteine of peroxiredoxins does not fully explain its unusually high reactivity with peroxide. Four conserved amino acids in the active site of all peroxiredoxins help stabilize the transition state of the peroxidatic S_n2 displacement reaction to enhance catalysis (43). This high reactivity with H_2O_2 together with their high abundance may explain the importance of Prdxs as redox sensors and transducers within cells. Andres-Mateos *et al.* (16) described DJ-1 as an "atypical peroxiredoxin-like peroxidase." They estimated that the reaction of H_2O_2 with DJ-1 was at least a thousand times slower than with typical Prdxs. Indeed, H_2O_2 reacted with DJ-1 at 0.56 ± 0.05 $M^{-1}\cdot s^{-1}$, whereas Prdxs reacted with the same substrate between 2×10^5 and 1.8×10^8 $M^{-1}\cdot s^{-1}$ (16, 44, 45). Due to the vastly different kinetics of these reactions, we suggest that H_2O_2 selectively oxidized Prdx, which acts as intracellular messenger of the oxidant signal by generating intermediate disulfide bond complexes with redox-sensitive proteins such as DJ-1. Thus, we propose a model in which the Cys-53 thiol of DJ-1 attacks the Prdx disulfide dimer, yielding a transitional trimeric intermediate. This trimeric

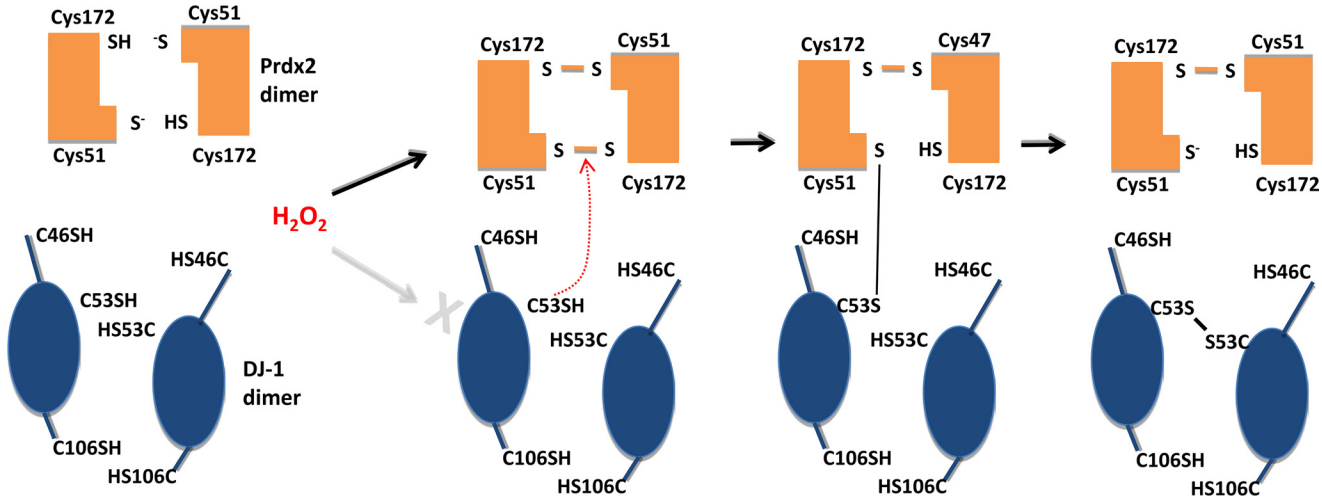

FIGURE 7. **Hypothetical model to explain H_2O_2-induced interaction of DJ-1 and Prdx2.** In the presence of H_2O_2 the peroxidatic cysteine of peroxiredoxin residue is oxidized to sulfenic acid, which then reacts with a free thiol of a resolving cysteine located in the other Prdx monomer. At this point DJ-1 Cys-53 attacks the peroxiredoxin disulfide dimer to yield a trimeric intermediate transition state. Thus, Prdx acts as a sensor and transducer of the oxidant signal by generating an intermediate disulfide bond complex with DJ-1. Finally, this trimeric structure is resolved to result in a homointerprotein disulfide bond between the Cys-53 residues from each DJ-1 monomer.

intermediate is abolished under higher levels of peroxide leading to the formation of DJ-1 disulfide dimer between the Cys-53 residues of both DJ-1 (Fig. 7). This model also explains the 75-kDa complex abrogation under high levels of peroxide, which is likely due to Prdx2 hyperoxidation.

Nuclear factor (erythroid-derived 2)-like 2 (Nrf2) activation has been associated with Prdx2 (46) and DJ-1 (47) in two independent studies. It is interesting to speculate that the disulfide interaction of Prdx2 and DJ-1 observed in this study could impact on Nrf2-dependent signaling, for example perhaps by modulating oxidation of the regulatory thiols in kelch-like ECH-associated protein 1 (keap1). The interaction of DJ-1 with Prdx1 and -6 has also been previously observed (48), although this was not increased by H_2O_2 treatment. A non-covalent association of DJ-1 and -6 would perhaps logically explain why it is able to form the heterodisulfide dimer, which is unlikely unless DJ-1 Cys-53 is very abundant and highly reactive. A non-covalent interaction of Prdx and DJ-1 may result from being similar-sized proteins, each from higher order oligomers. Indeed both Prdx and DJ-1 show overlap in function, each having both peroxidase (16, 25) and molecular chaperone activities (9, 22). The Cys-53 DJ-1-mediated interaction with Prdx2 is especially notable as most of the studies focus on Cys-106-mediated disulfide interactions with target proteins. However Cys-53 of DJ-1 is also known to be redox-regulated, with its reduction being mediated by Trx (49), which is consistent with our observation that Trx reductase inhibition by auranofin induces the disulfide dimer.

Oxidant-induced apoptosis has been widely observed to occur as either a cause or a consequence of distinct pathologies including cancer, autoimmune disease, neurodegeneration, and heart disease. This induction of apoptosis by oxidants is likely to be mediated, at least in part, by alterations to redox active proteins whose activity is modulated by such oxidative post-translational modifications. Prdxs are already known to induce disulfide bond formation in other proteins, thereby modulating their activities, for example protein disulfide isomerase (50), or STAT3 transcription factor (28). Here, we show that DJ-1 is also such a protein, undergoing complex, multifaceted, and dynamic redox-dependent alterations that are critical for induction of oxidant-induced apoptosis. The role of DJ-1 in cell death and apoptosis has been widely studied, with it complexing with several regulators of cell survival. Indeed, some of these proteins, such as ASK1 (14), Nrf2 (51), PTEN (52), and Akt (53), are also thiol redox state-regulated. Our data indicate that formation of DJ-1 Cys-106 disulfide linkage complexes is regulated by Cys-53 oxidation and that both cysteines are critical for the protective role of DJ-1. Additionally, we observed an oxidant-induced interaction between DJ-1 and Prdx2. This transient interaction between the two proteins may reflect an oxidant-sensing and transduction event, allowing post-translational regulation of DJ-1 function that is important in cellular responses to oxidative stress. Improving our understanding of the complexities of the redox regulation of DJ-1 is warranted as they may be important in the maintenance of health or the development of several diseases.

Author Contributions—P. E. conceived and coordinated the study and wrote the paper. M. F.-C. wrote the paper and designed, performed, and analyzed the experiments shown in Figs. 1–6. E. S. designed and developed the SO3H-Cys-106 DJ-1antibody and wrote the manuscript. H. C. designed and performed the flow cytometry experiments shown in Fig. 6. J. B. provided technical assistance with the expression of mutant proteins. J. B.-B. and M. M. provided technical assistance with the mass spectrometry analysis. All authors reviewed the final version of the manuscript.

References

1. Tao, X., and Tong, L. (2003) Crystal structure of human DJ-1, a protein associated with early onset Parkinson's disease. *J. Biol. Chem.* **278,** 31372–31379
2. Nagakubo, D., Taira, T., Kitaura, H., Ikeda, M., Tamai, K., Iguchi-Ariga, S. M., and Ariga, H. (1997) DJ-1, a novel oncogene which transforms mouse NIH3T3 cells in cooperation with ras. *Biochem. Biophys. Res. Commun.* **231,** 509–513

3. Bonifati, V., Rizzu, P., Squitieri, F., Krieger, E., Vanacore, N., van Swieten, J. C., Brice, A., van Duijn, C. M., Oostra, B., Meco, G., and Heutink, P. (2003) DJ-1(PARK7), a novel gene for autosomal recessive, early onset parkinsonism. *Neurol. Sci.* **24,** 159–160
4. Bonifati, V., Rizzu, P., van Baren, M. J., Schaap, O., Breedveld, G. J., Krieger, E., Dekker, M. C., Squitieri, F., Ibanez, P., Joosse, M., van Dongen, J. W., Vanacore, N., van Swieten, J. C., Brice, A., Meco, G., van Duijn, C. M., Oostra, B. A., and Heutink, P. (2003) Mutations in the DJ-1 gene associated with autosomal recessive early-onset parkinsonism. *Science* **299,** 256–259
5. Basak, I., Pal, R., Patil, K. S., Dunne, A., Ho, H. P., Lee, S., Peiris, D., Maple-Grødem, J., Odell, M., Chang, E. J., Larsen, J. P., and Møller, S. G. (2014) Arabidopsis AtPARK13, which confers thermotolerance, targets misfolded proteins. *J. Biol. Chem.* **289,** 14458–14469
6. Mitsugi, H., Niki, T., Takahashi-Niki, K., Tanimura, K., Yoshizawa-Kumagaye, K., Tsunemi, M., Iguchi-Ariga, S. M., and Ariga, H. (2013) Identification of the recognition sequence and target proteins for DJ-1 protease. *FEBS Lett.* **587,** 2493–2499
7. Chen, J., Li, L., and Chin, L. S. (2010) Parkinson disease protein DJ-1 converts from a zymogen to a protease by carboxyl-terminal cleavage. *Hum. Mol. Genet.* **19,** 2395–2408
8. Culleton, B. A., Lall, P., Kinsella, G. K., Doyle, S., McCaffrey, J., Fitzpatrick, D. A., and Burnell, A. M. (2015) A role for the Parkinson's disease protein DJ-1 as a chaperone and antioxidant in the anhydrobiotic nematode *Panagrolaimus superbus*. *Cell Stress Chaperones* **20,** 121–137
9. Girotto, S., Cendron, L., Bisaglia, M., Tessari, I., Mammi, S., Zanotti, G., and Bubacco, L. (2014) DJ-1 is a copper chaperone acting on SOD1 activation. *J. Biol. Chem.* **289,** 10887–10899
10. Cao, J., Ying, M., Xie, N., Lin, G., Dong, R., Zhang, J., Yan, H., Yang, X., He, Q., and Yang, B. (2014) The oxidation states of DJ-1 dictate the cell fate in response to oxidative stress triggered by 4-hpr: autophagy or apoptosis? *Antioxid. Redox Signal.* **21,** 1443–1459
11. Pantcheva, P., Elias, M., Duncan, K., Borlongan, C. V., Tajiri, N., and Kaneko, Y. (2014) The role of DJ-1 in the oxidative stress cell death cascade after stroke. *Neural Regen. Res.* **9,** 1430–1433
12. Milani, P., Ambrosi, G., Gammoh, O., Blandini, F., and Cereda, C. (2013) SOD1 and DJ-1 converge at Nrf2 pathway: a clue for antioxidant therapeutic potential in neurodegeneration. *Oxid. Med. Cell Longev.* **2013,** 836760
13. Joselin, A. P., Hewitt, S. J., Callaghan, S. M., Kim, R. H., Chung, Y. H., Mak, T. W., Shen, J., Slack, R. S., and Park, D. S. (2012) ROS-dependent regulation of Parkin and DJ-1 localization during oxidative stress in neurons. *Hum. Mol. Genet.* **21,** 4888–4903
14. Im, J. Y., Lee, K. W., Junn, E., and Mouradian, M. M. (2010) DJ-1 protects against oxidative damage by regulating the thioredoxin/ASK1 complex. *Neurosci Res* **67,** 203–208
15. Martinat, C., Shendelman, S., Jonason, A., Leete, T., Beal, M. F., Yang, L., Floss, T., and Abeliovich, A. (2004) Sensitivity to oxidative stress in DJ-1-deficient dopamine neurons: an ES- derived cell model of primary Parkinsonism. *PLoS Biol.* **2,** e327
16. Andres-Mateos, E., Perier, C., Zhang, L., Blanchard-Fillion, B., Greco, T. M., Thomas, B., Ko, H. S., Sasaki, M., Ischiropoulos, H., Przedborski, S., Dawson, T. M., and Dawson, V. L. (2007) DJ-1 gene deletion reveals that DJ-1 is an atypical peroxiredoxin-like peroxidase. *Proc. Natl. Acad. Sci. U.S.A.* **104,** 14807–14812
17. van der Brug, M. P., Blackinton, J., Chandran, J., Hao, L. Y., Lal, A., Mazan-Mamczarz, K., Martindale, J., Xie, C., Ahmad, R., Thomas, K. J., Beilina, A., Gibbs, J. R., Ding, J., Myers, A. J., Zhan, M., Cai, H., Bonini, N. M., Gorospe, M., and Cookson, M. R. (2008) RNA binding activity of the recessive parkinsonism protein DJ-1 supports involvement in multiple cellular pathways. *Proc. Natl. Acad. Sci. U.S.A.* **105,** 10244–10249
18. Canet-Avilés, R. M., Wilson, M. A., Miller, D. W., Ahmad, R., McLendon, C., Bandyopadhyay, S., Baptista, M. J., Ringe, D., Petsko, G. A., and Cookson, M. R. (2004) The Parkinson's disease protein DJ-1 is neuroprotective due to cysteine-sulfinic acid-driven mitochondrial localization. *Proc. Natl. Acad. Sci. U.S.A.* **101,** 9103–9108
19. Taira, T., Saito, Y., Niki, T., Iguchi-Ariga, S. M., Takahashi, K., and Ariga, H. (2004) DJ-1 has a role in antioxidative stress to prevent cell death. *EMBO Rep.* **5,** 213–218
20. Bandyopadhyay, S., and Cookson, M. R. (2004) Evolutionary and functional relationships within the DJ1 superfamily. *BMC Evol. Biol.* **4,** 6
21. Witt, A. C., Lakshminarasimhan, M., Remington, B. C., Hasim, S., Pozharski, E., and Wilson, M. A. (2008) Cysteine pKa depression by a protonated glutamic acid in human DJ-1. *Biochemistry* **47,** 7430–7440
22. Shendelman, S., Jonason, A., Martinat, C., Leete, T., and Abeliovich, A. (2004) DJ-1 is a redox-dependent molecular chaperone that inhibits α-synuclein aggregate formation. *PLoS Biol.* **2,** e362
23. Rehder, D. S., and Borges, C. R. (2010) Cysteine sulfenic acid as an intermediate in disulfide bond formation and nonenzymatic protein folding. *Biochemistry* **49,** 7748–7755
24. Wood, Z. A., Schröder, E., Robin Harris, J., and Poole, L. B. (2003) Structure, mechanism and regulation of peroxiredoxins. *Trends Biochem. Sci.* **28,** 32–40
25. Perkins, A., Nelson, K. J., Parsonage, D., Poole, L. B., and Karplus, P. A. (2015) Peroxiredoxins: guardians against oxidative stress and modulators of peroxide signaling. *Trends Biochem. Sci.* **40,** 435–445
26. Poynton, R. A., and Hampton, M. B. (2014) Peroxiredoxins as biomarkers of oxidative stress. *Biochim. Biophys. Acta* **1840,** 906–912
27. Zito, E., Melo, E. P., Yang, Y., Wahlander, Å., Neubert, T. A., and Ron, D. (2010) Oxidative protein folding by an endoplasmic reticulum-localized peroxiredoxin. *Mol. Cell* **40,** 787–797
28. Sobotta, M. C., Liou, W., Stöcker, S., Talwar, D., Oehler, M., Ruppert, T., Scharf, A. N., and Dick, T. P. (2015) Peroxiredoxin-2 and STAT3 form a redox relay for H_2O_2 signaling. *Nat. Chem. Biol.* **11,** 64–70
29. Gautier, C. A., Corti, O., and Brice, A. (2014) Mitochondrial dysfunctions in Parkinson's disease. *Rev. Neurol.* **170,** 339–343
30. Lev, N., Ickowicz, D., Barhum, Y., Melamed, E., and Offen, D. (2009) DJ-1 changes in G93A-SOD1 transgenic mice: implications for oxidative stress in ALS. *J. Mol. Neurosci.* **38,** 94–102
31. Lee, H., Choi, S. K., and Ro, J. Y. (2012) Overexpression of DJ-1 and HSP90α, and loss of PTEN associated with invasive urothelial carcinoma of urinary bladder: possible prognostic markers. *Oncol. Lett.* **3,** 507–512
32. Hod, Y. (2004) Differential control of apoptosis by DJ-1 in prostate benign and cancer cells. *J. Cell. Biochem.* **92,** 1221–1233
33. Miyajima, Y., Sato, Y., Oka, H., Utsuki, S., Kondo, K., Tanizaki, Y., Nagashio, R., Tsuchiya, B., Okayasu, I., and Fujii, K. (2010) Prognostic significance of nuclear DJ-1 expression in astrocytoma. *Anticancer Res.* **30,** 265–269
34. Niki, T., Takahashi-Niki, K., Taira, T., Iguchi-Ariga, S. M., and Ariga, H. (2003) DJBP: a novel DJ-1-binding protein, negatively regulates the androgen receptor by recruiting histone deacetylase complex, and DJ-1 antagonizes this inhibition by abrogation of this complex. *Mol. Cancer Res.* **1,** 247–261
35. Billia, F., Hauck, L., Grothe, D., Konecny, F., Rao, V., Kim, R. H., and Mak, T. W. (2013) Parkinson-susceptibility gene DJ-1/PARK7 protects the murine heart from oxidative damage *in vivo*. *Proc. Natl. Acad. Sci. U.S.A.* **110,** 6085–6090
36. Duan, X., Kelsen, S. G., and Merali, S. (2008) Proteomic analysis of oxidative stress-responsive proteins in human pneumocytes: insight into the regulation of DJ-1 expression. *J. Proteome Res.* **7,** 4955–4961
37. Kinumi, T., Kimata, J., Taira, T., Ariga, H., and Niki, E. (2004) Cysteine-106 of DJ-1 is the most sensitive cysteine residue to hydrogen peroxide-mediated oxidation *in vivo* in human umbilical vein endothelial cells. *Biochem. Biophys. Res. Commun.* **317,** 722–728
38. Meulener, M. C., Xu, K., Thomson, L., Thompson, L., Ischiropoulos, H., and Bonini, N. M. (2006) Mutational analysis of DJ-1 in *Drosophila* implicates functional inactivation by oxidative damage and aging. *Proc. Natl. Acad. Sci. U.S.A.* **103,** 12517–12522
39. Waak, J., Weber, S. S., Görner, K., Schall, C., Ichijo, H., Stehle, T., and Kahle, P. J. (2009) Oxidizable residues mediating protein stability and cytoprotective interaction of DJ-1 with apoptosis signal-regulating kinase 1. *J. Biol. Chem.* **284,** 14245–14257
40. Mitsumoto, A., Nakagawa, Y., Takeuchi, A., Okawa, K., Iwamatsu, A., and Takanezawa, Y. (2001) Oxidized forms of peroxiredoxins and DJ-1 on two-dimensional gels increased in response to sublethal levels of paraquat. *Free Radic. Res.* **35,** 301–310

41. Honbou, K., Suzuki, N. N., Horiuchi, M., Niki, T., Taira, T., Ariga, H., and Inagaki, F. (2003) The crystal structure of DJ-1, a protein related to male fertility and Parkinson's disease. *J. Biol. Chem.* **278,** 31380–31384
42. Aleyasin, H., Rousseaux, M. W., Phillips, M., Kim, R. H., Bland, R. J., Callaghan, S., Slack, R. S., During, M. J., Mak, T. W., and Park, D. S. (2007) The Parkinson's disease gene DJ-1 is also a key regulator of stroke-induced damage. *Proc. Natl. Acad. Sci. U.S.A.* **104,** 18748–18753
43. Hall, A., Nelson, K., Poole, L. B., and Karplus, P. A. (2011) Structure-based insights into the catalytic power and conformational dexterity of peroxiredoxins. *Antioxid. Redox Signal.* **15,** 795–815
44. Dubuisson, M., Vander Stricht, D., Clippe, A., Etienne, F., Nauser, T., Kissner, R., Koppenol, W. H., Rees, J. F., and Knoops, B. (2004) Human peroxiredoxin 5 is a peroxynitrite reductase. *FEBS Lett.* **571,** 161–165
45. Harrison, W. H., Whisler, W. W., and Hill, B. J. (1968) Catecholamine oxidation and ionization properties indicated from the H^+ release, tritium exchange, and spectral changes which occur during ferricyanide oxidation. *Biochemistry* **7,** 3089–3094
46. Matte, A., De Falco, L., Iolascon, A., Mohandas, N., An, X., Siciliano, A., Leboeuf, C., Janin, A., Bruno, M., Choi, S. Y., Kim, D. W., and De Franceschi, L. (2015) The interplay between peroxiredoxin-2 and nuclear factor-erythroid 2 is important in limiting oxidative mediated dysfunction in β-thalassemic erythropoiesis. *Antioxid. Redox Signal.* **23,** 1284–1297
47. Clements, C. M., McNally, R. S., Conti, B. J., Mak, T. W., and Ting, J. P. (2006) DJ-1, a cancer- and Parkinson's disease-associated protein, stabilizes the antioxidant transcriptional master regulator Nrf2. *Proc. Natl. Acad. Sci. U.S.A.* **103,** 15091–15096
48. Knobbe, C. B., Revett, T. J., Bai, Y., Chow, V., Jeon, A. H., Böhm, C., Ehsani, S., Kislinger, T., Mount, H. T., Mak, T. W., St George-Hyslop, P., and Schmitt-Ulms, G. (2011) Choice of biological source material supersedes oxidative stress in its influence on DJ-1 *in vivo* interactions with Hsp90. *J. Proteome Res.* **10,** 4388–4404
49. Fu, C., Wu, C., Liu, T., Ago, T., Zhai, P., Sadoshima, J., and Li, H. (2009) Elucidation of thioredoxin target protein networks in mouse. *Mol. Cell. Proteomics* **8,** 1674–1687
50. Tavender, T. J., Springate, J. J., and Bulleid, N. J. (2010) Recycling of peroxiredoxin IV provides a novel pathway for disulphide formation in the endoplasmic reticulum. *EMBO J.* **29,** 4185–4197
51. Liu, C., Chen, Y., Kochevar, I. E., and Jurkunas, U. V. (2014) Decreased DJ-1 leads to impaired Nrf2-regulated antioxidant defense and increased UV-A-induced apoptosis in corneal endothelial cells. *Invest. Ophthalmol. Vis. Sci.* **55,** 5551–5560
52. Klawitter, J., Klawitter, J., Agardi, E., Corby, K., Leibfritz, D., Lowes, B. D., Christians, U., and Seres, T. (2013) Association of DJ-1/PTEN/AKT- and ASK1/p38-mediated cell signalling with ischaemic cardiomyopathy. *Cardiovasc. Res.* **97,** 66–76
53. Zhu, Z. M., Li, Z. R., Huang, Y., Yu, H. H., Huang, X. S., Yan, Y. F., Shao, J. H., and Chen, H. P. (2014) DJ-1 is involved in the peritoneal metastasis of gastric cancer through activation of the Akt signaling pathway. *Oncol. Rep.* **31,** 1489–1497